

## Review

# Proposed Neuroimaging Criteria for the Diagnosis of Multiple System Atrophy

David J. Brooks, MD, Dsc, FRCP<sup>1\*</sup> and Klaus Seppi MD<sup>2</sup> for the Neuroimaging Working Group on MSA

<sup>1</sup>Division of Neuroscience, Faculty of Medicine, Imperial College London, London, United Kingdom

<sup>2</sup>Department of Neurology, University of Innsbruck, Innsbruck, Austria

---

**Abstract:** In this article, we review the state of the art knowledge concerning structural and functional imaging in multiple system atrophy (MSA). The relative value of imaging modalities in the differential diagnosis of MSA from other parkinsonian syndromes is debated. It is concluded that, although neu-

roimaging biomarkers provide valuable supportive data alongside clinical assessments, it is not possible to use them as surrogate markers. © 2009 Movement Disorder Society

**Key words:** multiple system atrophy; Parkinson; MRI; PET; SPECT

---

Multiple system atrophy (MSA) includes Shy-Drager syndrome, striatonigral degeneration (SND or MSA-P), and sporadic olivopontocerebellar atrophy (sOPCA or MSA-C) within its spectrum. It is characterized pathologically by argyrophilic,  $\alpha$ -synuclein positive inclusions in glia and neurones in substantia nigra (SN), striatum, brainstem and cerebellar nuclei, and intermediolateral columns of the cord. Current consensus guidelines concerning the diagnosis of MSA do not include imaging findings—they are purely based on clinical criteria. In this presentation, the potential value and role of neuroimaging are presented and discussed. Indeed, revised consensus criteria now include neuroimaging criteria for the diagnostic category of possible MSA.

## STRUCTURAL IMAGING IN MSA

Several studies on the diagnostic accuracy of structural imaging methods have been published in this field over the past two decades. Those studies summarized in Tables 1–4 have included at least 10 subjects with MSA and at least 10 subjects in the comparison groups. Patients had to be diagnosed using established diagnostic criteria and data presented in sufficient detail to allow calculation of sensitivities and specificities. In addition, the same MR protocol or at least MR scanner or same field strength had to be used throughout a study. If a study used different MR protocols or different field strengths, the study was not included into the table.

### Conventional MRI

Abnormalities on conventional MRI at 1.5 T in patients with MSA may include not only putaminal abnormalities such as atrophy, T2 hypointensity, and “slit-like” marginal hyperintensity but also atrophy of the lower brainstem, middle cerebellar peduncles (MCPs), and cerebellum, as well as hyperintensities in the pons, MCPs, and cerebellum.<sup>1,2,7,12,24–28</sup> Although putaminal atrophy appears to discriminate MSA from PD, T2 putaminal hypointensity and a putaminal hyperintense rim may also occur in the latter (see

---

This article is part of the journal's online CME program. The CME activity including form, can be found online at <http://www.movementdisorders.org/education/journalcme/>

\*Correspondence to: David J. Brooks, Division of Neuroscience, Faculty of Medicine, Imperial College London, London, United Kingdom. E-mail: david.brooks@csc.mrc.ac.uk

Potential conflict of interest: DJB works for GE health care. KS has no disclosure.

Received 30 August 2007; Revised 30 October 2008; Accepted 5 November 2008

Published online 20 March 2009 in Wiley InterScience (www.interscience.wiley.com). DOI: 10.1002/mds.22413

TABLE 1. Diagnostic accuracy of conventional MRI for the diagnosis of MSA

Author/Year	Cohort size	Diagnostic predictor	Sensitivity (%)	Specificity (%)
Konagaya et al., 1994 <sup>1</sup>	MSA 28/PD 25	Putaminal rim	61	100
Kraft et al., 1999 <sup>2</sup>	MSA-P 15/PD 65/PSP 10	Putaminal rim Putaminal signal changes at T2 Putaminal rim and hypointense putamen	61	100
von Lewinski et al., 2007 <sup>3</sup>	MSA 52/PD 88/HC 29	Hypointense putamen Putaminal signal changes using T2* GE sequences Signal loss dorsolateral putamen	64	100
Righini et al., 2002 <sup>4</sup>	MSA-P 24/PD 27	Signal loss dorsolateral putamen and hyperintense putaminal rim S <sub>PUT/CAUD</sub> Putaminal signal changes on FSE and CSE	36	91 vs. PD/60 vs. PSP
Schocke et al., 2002 <sup>5</sup>	MSA-P 10/PD 11/HC 7	FSE CSE (proton density—putaminal hyperintensity) CSE (T2—putaminal hypointensity) Putaminal abnormalities at T2	69	91 vs. PD
Lee et al., 2004 <sup>6</sup>	MSA-P 36/MSA-C 27/PD 30	Putaminal rim 10 supra- and infratentorial MRI findings characteristic for MSA; findings with the highest sensitivity (>70%) are given below; specificity values vs. PD are given	42	97 vs. PD
Bhattacharya et al., 2002 <sup>7</sup>	MSA-P 14/MSA-C 4/PD 21	Putaminal atrophy Putaminal hypointensity Putaminal rim Dilatation 4th ventricle MCP atrophy Pontine atrophy Cerebellar atrophy Signal increase cerebellum Signal increase MCP Several putaminal and infratentorial abnormalities on MRI; significant MRI findings differentiating MSA-P from PD are given below	65	95 vs. PD
Burk et al., 2005 <sup>8</sup>	MSA-C 30/IDCA-P 11	Putaminal rim Putaminal signal changes on FSE and CSE FSE CSE (proton density—putaminal hyperintensity) CSE (T2—putaminal hypointensity) Putaminal abnormalities at T2 Putaminal atrophy Putaminal rim 10 supra- and infratentorial MRI findings characteristic for MSA; findings with the highest sensitivity (>70%) are given below; specificity values vs. PD are given	80	91 vs. PD/100 vs. HC
		Putaminal hypointensity Putaminal atrophy Putaminal rim Dilatation 4th ventricle MCP atrophy Pontine atrophy Cerebellar atrophy Signal increase cerebellum Signal increase MCP Several putaminal and infratentorial abnormalities on MRI; significant MRI findings differentiating MSA-P from PD are given below	90 (MSA-P)/82 (MSA-C) 83 (MSA-P) 72 (MSA-P) 78 (MSA-P)/93 (MSA-C) 75 (MSA-P)/100 (MSA-C) 100 (MSA-C) 96 (MSA-C) 82 (MSA-C) 85 (MSA-C)	70 87 90 87 87 87 90 97 100
		Putaminal atrophy Putaminal hypointensity (moderate/severe) Putaminal rim (moderate/severe) Midbrain atrophy Pontine atrophy Atrophy medulla oblongata Signal increase MCP Hot cross bun sign Several supra- and infratentorial MRI findings characteristic for MSA; significant MRI findings differentiating MSA-C from IDCA-P are given below	43 43 36 36 43 43 21 7	100 100 95 100 100 100 100 100
		MCP atrophy Brainstem atrophy Hypointensity dentate nuclei Hot cross bun sign Hyperintensity MCP	93 100 57 97 87	82 82 100 100 100

TABLE 1. (Continued)

Author/Year	Cohort size	Diagnostic predictor	Sensitivity (%)	Specificity (%)
Nicoletti et al., 2006 <sup>9</sup>	MSA 16 (MSA-P in 13)/PD 26/ HC 14	Putaminal atrophy, putaminal hypointensity, putaminal rim, brainstem atrophy, hyperintensity of the MCP, and cruciform hyperintensity of the pons; significant MRI findings differentiating MSA-P from PD and HC are given below		
		Putaminal hypointensity	38	100
		Putaminal rim	56	96 vs. PD/100 vs. HC
		Hot cross bun sign	50	100
		Presence of at least one of the abnormal features mentioned earlier	100	96 vs. PD/100 vs. HC
Paviour et al., 2007 <sup>10</sup>	MSA-P 11/PD 12/PSP 20/HC 7	Putaminal rim, putaminal hypointensity, signal increases in MCP and pons		
		Putaminal hypointensity	27	100 vs. PD/80 vs. PSP
		Putaminal rim	55	83 vs. PD/90% vs. PSP
		Signal increase pons	45	100 vs. all groups
		Signal increase MCP	36	100 vs. all groups
		Putaminal abnormalities		
		Putaminal rim (moderate/severe)	47	100 (vs. PD and HC)
		Putaminal hypointensity (moderate/severe)	47	100 (vs. PD and HC)
		Putaminal atrophy	67	100 (vs. PD and HC)
Seppi et al., 2006 <sup>11</sup>	MSA-P 15/PD 20/HC 11			

MSA, multiple system atrophy; PD, Parkinson's disease; PSP, progressive supranuclear palsy; HC, healthy controls; GE, gradient echo; SI<sub>PUT/CAUD</sub>, signal intensity (SI) dorsolateral putamen/SI head of caudate nucleus; FSE, fast spin echo; CSE, conventional spin echo; MCP, middle cerebellar peduncle; IDCA-P, idiopathic cerebellar ataxia with extracerebellar presentation not corresponding to MSA-C; SCP, superior cerebellar peduncle.

All but one study<sup>9</sup>, which was performed at 1.0 T, were performed at 1.5 T.

Table 1).<sup>5,7,29-31</sup> In fact, on T2-weighted images at 3.0 T, a hyperintense putaminal rim is a nonspecific, normal finding.<sup>32</sup> Signal hyperintensities within the pons and MCPs in MSA may occasionally result in the “hot-cross bun” sign (Fig. 1) and, while a feature of MSA, may occur also in patients with Parkinsonism because of other causes.<sup>33,34</sup>

Overall, the specificity of the MRI signal changes and atrophy at 1.5 T associated with MSA in putamen and infratentorial structures<sup>2,5,7,12,24-28</sup> compared with PD or healthy controls is high,<sup>5-7,26</sup> but their reported sensitivity to detect MSA is inconsistent in the literature and suboptimal in the early disease stages (Fig. 2 and 3).<sup>5,6,28,35,36</sup> A recent study in fact suggests a positive association between disease duration and signal abnormalities in the pons as well as in the putamen in MSA.<sup>37</sup> Sensitivity can be somewhat improved by modifying technical aspects such as slice thickness and the use of conventional spin-echo (CSE) or T2\*-weighted gradient echo sequences.<sup>3-5,38</sup> The specificity of conventional MRI for discriminating MSA from other types of APS is suboptimal<sup>27,30</sup> (Table 1).

Evidence supporting a role for conventional MRI in the diagnosis of MSA-C is scarce. Burk et al.<sup>8</sup> investigated the discriminative validity of conventional MRI (cMRI) at 1.5 T in patients with sporadic cerebellar ataxia including patients with MSA-C and patients with idiopathic cerebellar ataxia and Parkinsonism (IDCA-P). Patients with MSA-C were characterized by a higher frequency and severity of MRI abnormalities (atrophic changes and additional hyperintense signal changes) of the MCP and pons. The presence of these MRI features thus points to the diagnosis of MSA-C and helps differentiate MSA-C from other types of sporadic cerebellar ataxia with extracerebellar features (Table 1).

#### Quantitative Assessment of Regional Cerebral Atrophy Using MRI Planimetry and Volumetry

Using MRI volumetry (MRV) with semiautomatic segmentation techniques with a region-of-interest (ROI) approach at 1.5 T, volume loss of different supratentorial and infratentorial brain structures, including striatum, brainstem, and cerebellum, has been reported in patients with MSA<sup>12,39</sup>. On the basis of individual structure volumetry, differentiation of MSA from other parkinsonian disorders is scarce.<sup>12</sup> Application of a stepwise discriminant analysis in patients with MSA, PSP, PD, and healthy controls allowed discrimination of all 12 patients with MSA-P and 15 of 17 patients with MSA-C from the PD patients and healthy controls, whereas differentiation of patients with MSA from PSP was poor<sup>12</sup> (Table 2).

**TABLE 2.** Diagnostic accuracy of MRI methods for the quantitative assessment of regional cerebral atrophy including MR-planimetry/volumetry for the diagnosis of MSA

Author/Year	Cohort size	Diagnostic predictor	Sensitivity (%)	Specificity (%)
Schulz et al., 1999 <sup>12</sup>	MSA-P 12/MSA-C 17/PD 11/PSP 6/HC 16	Atrophy of the caudate nucleus, putamen, brainstem, and cerebellum using MRV Model including volumes of brainstem, caudate nucleus, putamen, cerebellum (using stepwise linear discrimination model) <sup>a</sup>	67 (MSA-P)/ 76 (MSA-C)	100 (MSA-P vs. PD)/ 100 (MSA-P vs. HC)/ 67 (MSA-P vs. PSP)/ 100 (MSA-C vs. PD)/ 82 (MSA-C vs. HC)/100 (MSA-C vs. PSP)
Burk et al., 2004 <sup>13</sup>	MSA-C 33/IDCA-P 13/HC 16	Atrophy of the caudate nucleus, putamen, brainstem, and cerebellum using MRV. Model including volumes of cerebellum, brainstem, caudate nucleus and putamen, (using stepwise linear discrimination model) <sup>b</sup>	82	100
Nicoletti et al., 2006 <sup>9</sup>	MSA 16 (MSA-P in 13)/PD 26/HC 14	MCP width on T1 MCP with <8 mm	100	100
Quattrone et al., 2008 <sup>14</sup>	MSA-P 19/PD 108/PSP 33/HC 50	Single and combined quantitative imaging measurements of brain structures on T1: midbrain area (M), pontine area (P), MCP width (MCP), SCP width (SCP). Sensitivity and specificity given only compared with PSP. P/M ratio MCP/SCP ratio MR parkinsonism index = (P/M)*(MCP/SCP)	95 90 100	97 94 100

<sup>a</sup>No PD patient was classified as having MSA-P or vice-versa; however, 3 of the PD patients were classified as having MSA-C or PSP; discrimination of patients with MSA from PSP was poor.

<sup>b</sup>There was substantial cerebellar atrophy in both cerebellar groups, whereas additional brainstem atrophy was significantly more pronounced in MSA-C patients. Absolute caudate and putamen atrophy was found to be restricted to single MSA-C individuals, whereas group comparisons of mean volumes did not yield significant differences from controls. One control subject (6%) and 6 MSA-C patients (18%) were classified as IDCA-P.

MSA, multiple system atrophy; PD, Parkinson's disease; PSP, progressive supranuclear palsy; HC, healthy controls; IDCA-P, idiopathic cerebellar ataxia with extracerebellar presentation not corresponding to MSA-C; MCP, middle cerebellar peduncle; SCP, superior cerebellar peduncle.

All studies were performed at 1.5 T.

Burk et al.<sup>13</sup> used MRV with ROIs to study the atrophy of the cerebellum, brainstem, caudate nucleus, and putamen, in patients with sporadic cerebellar ataxia (including patients with MSA-C and IDCA-P) compared with control subjects. By application of stepwise discriminant analysis, diagnosis could be correctly predicted in 94% of the controls, 82% of the MSA-C patients, and 100% of the IDCA-P patients (Table 2).

More recently, studies using voxel-based morphometry (VBM) have been performed in patients with MSA confirming previous ROI-based volumetric studies showing basal ganglia and infratentorial volume loss in MSA patients<sup>40-45</sup> with structural abnormalities in infratentorial brain regions being more pronounced in MSA-C than in MSA-P patients.<sup>44</sup> Furthermore, these data also revealed volume loss in several cortical regions in patients with MSA-P and MSA-C. However, VBM is not appropriate for routine diagnostic work-up of individual patients.

As an indirect measure of brain structures known to be atrophic in MSA, groups have applied simple quantitative measures of diameters and areas of different structures on MRI for the differential diagnosis of MSA from other neurodegenerative parkinsonian disorders. The average MCP width was shown to be significantly smaller in patients with MSA than in those with PD or control subjects without any overlap between MSA patients and PD patients or healthy subjects.<sup>9</sup> The separation of MSA from PSP patients, however, was suboptimal.<sup>9,14</sup> (Table 2) Consistent with the well-known atrophy of the pons in MSA, the area of the pons measured on midsagittal T1-weighted MR images has been shown to be significantly smaller in MSA-P patients compared with patients with PD and PSP as well as healthy controls with overlapping individual values.<sup>14,46</sup> On the other hand, midbrain areas measured on midsagittal T1-weighted MR images are significantly smaller in PSP patients compared with

**TABLE 3.** Diagnostic accuracy of quantitative structural MR-based techniques including diffusion-weighted MR and magnetization transfer imaging for the diagnosis of MSA

Author/Year	Cohort size	Diagnostic predictor	Sensitivity (%)	Specificity (%)
Schocke et al., 2002 <sup>5</sup>	MSA-P 10/PD 11/HC 7	ADCs in the basal ganglia, pons, white matter; sensitivity and specificity values given for putaminal ADCs (best discriminator)		
		Putaminal ADCs > 0.760 × 10 <sup>3</sup> mm <sup>2</sup> /s	100	100 (vs. PD and HC)
Seppi et al., 2004 <sup>15</sup>	MSA-P 15/PD 17/HC 10 including all patients studied by Schocke et al., 2002	Striatal ADCs Striatal ADCs > 0.795 × 10 <sup>3</sup> mm <sup>2</sup> /s	93	100 (vs. PD and HC)
Schocke et al., 2004 <sup>16</sup>	MSA-P 11/PD 17/HC 10	Putaminal ADC values Putaminal ADC > 0.80 × 10 <sup>3</sup> mm <sup>2</sup> /s	100	100 (vs. PD and HC)
Seppi et al., 2006 <sup>11</sup>	MSA-P 15/PD 20/HC 11 including all patients studied by Schocke et al., 2004	Putaminal ADC values of the whole, anterior and posterior putamen Putaminal ADC > 0.80 × 10 <sup>3</sup> mm <sup>2</sup> /s Posterior putaminal ADC > 0.80 × 10 <sup>3</sup> mm <sup>2</sup> /s	93 100	100 (vs. PD and HC) 100 (vs. PD and HC)
Nicoletti et al., 2006 <sup>17</sup>	MSA-P 16/PD 16/PSP 16/HC 15	ADC values in the basal ganglia, pons, white matter; sensitivity and specificity values given for putaminal and MCP diffusivity (best discriminators) MCP ADC > 0.875 × 10 <sup>3</sup> mm <sup>2</sup> /s Putaminal ADC > 0.953 × 10 <sup>3</sup> mm <sup>2</sup> /s	100 100	100 (vs. all groups) 100 (vs. PD and HC)/ 81 (vs. PSP)
Paviour et al., 2007 <sup>10</sup>	MSA-P 11/PD 12/PSP 20/HC 7	ADC values in the basal ganglia, pons, MCP, SCP, thalamus; sensitivity and specificity values given for MCP diffusivity (in the article) MCP ADC > 0.733 × 10 <sup>3</sup> mm <sup>2</sup> /s	91	82 (vs. all groups)/ 84 (vs. PSP)
Ito et al., 2007 <sup>18</sup>	MSA 20 (MSA-P 10)/PD 21/HC 20	FA and ADC in the pons, cerebellum and putamen at 3.0T; sensitivity and specificity values given for MSA-P vs. PD ADC pons > 0.98 × 10 <sup>3</sup> mm <sup>2</sup> /s ADC cerebellum > 0.96 × 10 <sup>3</sup> mm <sup>2</sup> /s ADC putamen > 0.83 × 10 <sup>3</sup> mm <sup>2</sup> /s FA pons < 0.38 FA cerebellum < 0.30 FA putamen < 0.35 both low FA and high ADC values in any of the three areas	70 60 70 70 70 70 90	70 88 64 100 64 88 100
Eckert et al., 2004 <sup>19</sup>	MSA 12/PD 15/PSP 10/HC 20	MTR in the globus pallidus, putamen, caudate nucleus, SN, and white matter <sup>a</sup> Model including MTRs of globus pallidus, putamen and caudate nucleus (using stepwise linear discrimination model)	58	100 (vs. PD and HC)/ 90 (vs. PSP)

<sup>a</sup>The main finding in this study was a change in the MT ratio (MTR) in the globus pallidus, putamen, caudate nucleus, substantia nigra, and white matter in PD, MSA, and PSP patients, matching the pathological features of the underlying disorder. MTRs were significantly reduced in the putamen in MSA patients compared with PD patients and healthy controls as well as in the substantia nigra in patients with PSP, MSA, and PD.

MSA, multiple system atrophy; PD, Parkinson's disease; HC, healthy controls; ADC, apparent diffusion coefficient—in the studies by Schocke et al., 2002 and Seppi et al., 2004 measured in z-slice direction only, in the other studies ADCs were averaged over three orthogonal measurements, thus representing the trace of the diffusion tensor; PSP, progressive supranuclear palsy; MCP, middle cerebellar peduncle; SCP, superior cerebellar peduncle; FA, fractional anisotropy; MTR, magnetization transfer ratio; SN, substantia nigra.

All but one study<sup>18</sup>, which was performed at 3.0 T, were performed at 1.5 T.

healthy controls and patients with PD and MSA-P.<sup>14,46</sup> Calculation of the ratio between pontine and midbrain areas discriminated completely MSA-P patients from patients with PD and PSP and healthy controls in one series,<sup>46</sup> though in another individual values overlapped.<sup>14</sup> For this reason, Quattrone proposed an

index termed the MR Parkinsonism index (MRPI), which was calculated by multiplying the pontine area-midbrain area ratio (P/M) by the MCP width-SCP width ratio (MCP/SCP) [(P/M)\*(MCP/SCP)]. (Table 2) The MRPI value was significantly higher in patients with PSP than in patients with PD and MSA-P as well

**TABLE 4.** Diagnostic accuracy of transcranial sonography for the diagnosis of MSA

Author/Year	Cohort size	Diagnostic predictor	Sensitivity (%)	Specificity (%)
Walter et al., 2003 <sup>20</sup>	MSA 16/PD 25/PSP 9	Hyperechogenicity of the SN and LN (hyperechogenic if it was more intense than the surrounding white matter)	94 (for MSA)/ 91 (for APS)	96 (vs. PD)
		SN echogenicity (<0.2 cm <sup>2</sup> )	100	76 (vs. PD)
Behnke et al., 2005 <sup>21</sup>	MSA-P 32/PD 88/PSP 18	SN echogenicity (<0.25 cm <sup>2</sup> )	77 (for APS)	77 (vs. PD)
		LN hyperechogenicity		
		Hyperechogenicity of the SN (>80th percentile of controls) and LN		
		Absent uni-/bilateral SN hyperchogenicity	70 (for MSA-P)/ 70 (for APS)	89 (vs. PD)
Okawa et al., 2007 <sup>22</sup>	MSA 14/PD 98/PSP 17/HC 30	Uni-/bilateral LN hyperechogenicity	72 (for MSA-P)/ 72 (for APS)	89 (vs. PD)
		Combination of absent SN hyperchogenicity and uni-/bilateral LN hyperechogenicity	56 (for APS)	93 (vs. PD)
		Combination of unilateral SN hyperchogenicity and regular bilateral LN echogenicity	88 (for APS)	66 (vs. PD)
Walter et al., 2007 <sup>23</sup>	MSA-P 21/PD 138/PSP 22	Hyperechogenicity of the SN (greater value of bilateral measurements was considered): normal echogenicity; moderate hyperechogenicity; marked hyperechogenicity; hyperechogenicity of LN (hyperechogenic if it was more intense than the surrounding white matter); 3rd ventricle dilatation—not given here, because it is a characteristic for PSP patients <sup>a</sup>	91 (for MSA), 92 (for APS)	83 (vs. PD)
		Normal SN echogenicity	90 (for MSA-P), 72 (for APS)	98 (vs. PD)
		Normal SN echogenicity with hyperechogenic LN	65 (for MSA-P), 59 (for APS)	100 (vs. PD)
		Normal/moderate SN hyperechogenicity with hyperechogenic LN	77 for APS	97 (vs. PD)

<sup>a</sup>Semiquantitative grading of the SN hyperechogenicity was performed based on SN echogenicity values of 300 healthy controls: normal SN echogenicity corresponding to a SN area <0.2 cm<sup>2</sup>, i.e., <75th percentile; moderate SN hyperechogenicity corresponding to a SN area of 0.2 cm<sup>2</sup> or larger and <0.25 cm<sup>2</sup>, i.e., 75th–90th percentile; marked SN hyperechogenicity corresponding to a SN area of 0.25 cm<sup>2</sup> or larger, i.e., >90th percentile of HC.

MSA, multiple system atrophy; PD, Parkinson's disease; PSP, progressive supranuclear palsy; SN, substantia nigra; LN, lentiform nucleus; HC, healthy controls.

as control participants, with no patient with PSP receiving a misdiagnosis when the index was used.

#### Quantitative Structural MR-Based Techniques: Diffusion-Weighted Imaging and Magnetization Transfer Imaging

Diffusion-weighted (DWI) and magnetization transfer (MTI) imaging potentially represent useful diagnostic tools that can provide additional support for a diagnosis of MSA-P.<sup>5,10,11,15–19,47–50</sup>

Different groups<sup>5,11,16,17,47</sup> have been reported that DWI at 1.5 T is able to discriminate patients with MSA-P and both healthy volunteers and patients with PD on the basis of putaminal ADC and Trace(D) values. The finding of increased putaminal diffusivity in

patients with MSA-P has been reproduced, although one study<sup>10</sup> with methodological limitations regarding acquisition and segmentation of the DWI images could not confirm this. In line with the known underlying neuropathology in MSA-P, a more severe involvement of posterior compared with anterior putaminal diffusivity was found in patients with MSA-P.<sup>11</sup> Although putaminal diffusivity overlapped in MSA-P and PSP patients, diffusivity in the MCP has been shown to be higher in patients with MSA-P compared with PSP, allowing a good discrimination between these two disease entities.<sup>10,17</sup> In a further study, an increase of ADCs was found in the pons, MCP, cerebellar white matter, and putamen of MSA-C patients compared with controls.<sup>49</sup> DWI proved superior to searching for the presence of supratentorial (mainly putaminal)<sup>5,17,29</sup>

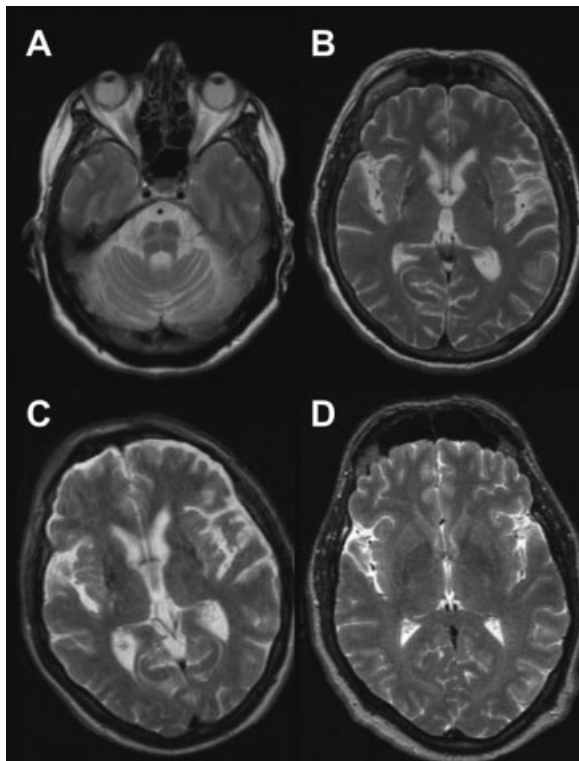


**FIG. 1.** A: Hot cross bun in a patient with MSA-C (women 62 years; disease duration 3 years; Hoehn and Yahr stage 3) on T2-weighted images (1.5 T whole-body MR scanner). B: Putaminal changes (hyperintense rim, putaminal hypointensity in comparison with the globus pallidus and putaminal atrophy) at both sides in a patient with MSA-P (women; age 66 years; disease duration 4 years; Hoehn and Yahr stage 3) on T2-weighted images (1.5 T whole-body MR scanner). C: Putaminal changes (hyperintense rim accentuated at left side, putaminal hypointensity in comparison with the globus pallidus and putaminal atrophy at both sides) in a patient with MSA-C (men; age 64 years; disease duration 3.5 years; Hoehn and Yahr stage 4) on T2-weighted images (1.5 T whole-body MR scanner). D: No relevant abnormalities in the basal ganglia in a patient with PD (women; age 58 years; disease duration 5 years; Hoehn and Yahr stage 2) on T2-weighted images (1.5 T whole-body MR scanner).

and infratentorial abnormalities<sup>17</sup> on MRI when discriminating MSA-P from PD. Paviour et al.<sup>10</sup> found that ADCs in the putamen or in the SCP did not differ between patients with MSA and patients with PD or PSP. This clearly contrasts with previous reports showing significantly increased putaminal diffusivity in patients with MSA-P<sup>5,6,11,16,17</sup> and significant decreased ADCs in the SCP in PSP patients<sup>50</sup> at 1.5 T. Methodological and demographic reasons may explain this. Disease durations especially of the PD group in the article by Paviour et al. were longer than in the previous articles. The DWI MR protocol with a slice thickness of 7 mm compared with 3 to 5 mm used in other studies<sup>15,17,18,50</sup> might be inadequate. Further-

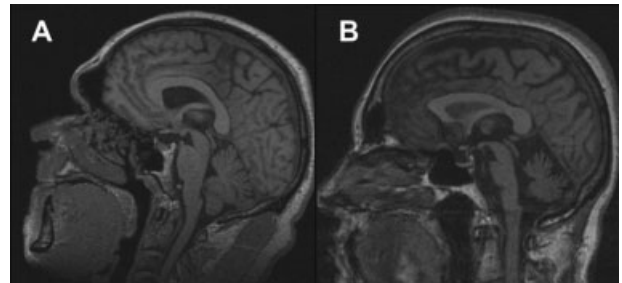


**FIG. 2.** A: No relevant brainstem atrophy in a patient with PD (men; age 55 years; disease duration 5 years; Hoehn and Yahr stage 2) on midsagittal T1-weighted image (1.5 T whole-body MR scanner). B: Infratentorial atrophy (pons and cerebellum; dilated fourth ventricle) in a patient with MSA-P (women; age 61 years; disease duration 3.5 years; Hoehn and Yahr stage 3) on midsagittal T1-weighted image (1.5 T whole-body MR scanner).

more, segmentation errors may have occurred; in the published figure displaying the ROIs, the delineated ROI of the putamen contains clearly the parts of globus pallidus.

Ito et al.<sup>18</sup> compared diffusivity and fractional anisotropy (FA) values in the pons, cerebellum, and putamen of patients with MSA and PD as well as controls using a 3.0 T MR system. Diffusivity values in the pons, cerebellum, and putamen were significantly

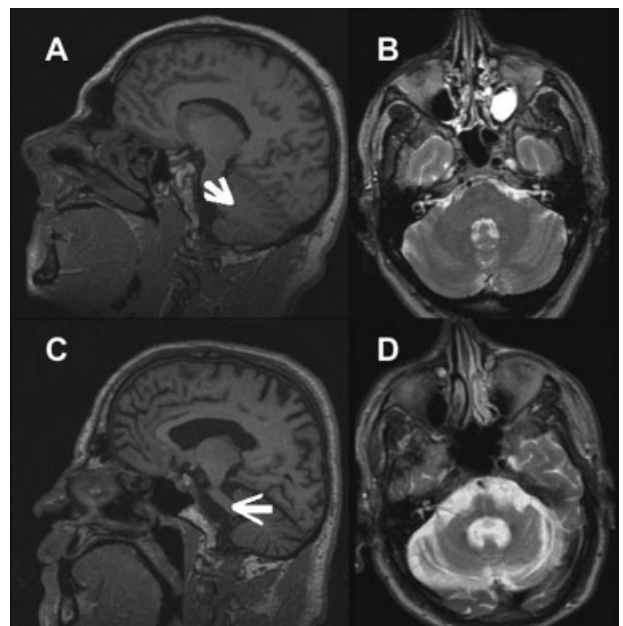


**FIG. 3.** A, B: No relevant atrophy of the middle cerebellar peduncle (arrow) in a patient with PD (men; age 55 years; disease duration 5 years; Hoehn and Yahr stage 2) on sagittal T1-weighted images and on axial T2-weighted images (1.5 T whole-body MR scanner). C, D: Atrophy of the middle cerebellar peduncle (arrow) in a patient with MSA-P (women; age 61 years; disease duration 4 years; Hoehn and Yahr stage 3) on sagittal T1-weighted images and on axial T2-weighted images (1.5 T whole-body MR scanner).

higher, and FA values lower in MSA than in PD or controls. Using FA and diffusivity values to differentiate MSA-P from PD yielded equal sensitivity (70%) and higher specificity (100%) for the pons than the putamen and cerebellum. In addition, all patients that had both significant low FA and high diffusivity values in each of these three areas were MSA-P cases, and those that had both normal FA and diffusivity values in the pons were all PD cases.

Basal ganglia abnormalities have also been reported in patients with MSA-P when studied with MTI.<sup>19,48</sup> By application of stepwise discriminant analysis of MT ratios in the basal ganglia and SN, there was a good discrimination of PD patients and controls from the MSA and PSP patients with only 1 MSA patient wrongly classified into the control group, whereas separation between PD patients and controls and between MSA and PSP patients was suboptimal.<sup>19</sup>

### Transcranial Sonography

In recent years, transcranial sonography (TCS) has become a widely used method for the visualization of the brain parenchyma through the intact skull. Using TCS, recent studies have reported midbrain hyperechogenicity in the area of the SN in 80 to 90% of patients with PD, but also in about 10% of healthy adult controls and patients with atypical Parkinsonism due to MSA and PSP.<sup>20–23,51–53</sup> Conversely, unilateral or bilateral hyperechogenicity of the lentiform nucleus (LN) can be detected in at least 70% of patients with atypical Parkinsonism due to MSA or PSP and in around one-quarter of patients with PD.<sup>20,21,23</sup> Combining a hyperechogenic LN with a nonmarked echogenic SN appears specific for atypical parkinsonian patients with MSA and PSP though sensitivity is suboptimal.<sup>21,23</sup>

Advantages of brain parenchyma sonography with TCS are that it is easy accessible and less-expensive compared with other imaging modalities, such as functional imaging with SPECT/PET or MRI. On the other hand, TCS has technical limitations. There is no temporal bone window in about 10 to 15% of the subjects, thus not allowing the application of the method in these subjects. Furthermore, hyperechogenicity in brain parenchyma is not quantifiable leading to a certain degree of subjectivity when reporting.

## FUNCTIONAL IMAGING IN MSA

### FDG PET Studies in MSA

A number of FDG PET series have examined the different patterns of resting regional cerebral glucose

metabolism associated with variants of MSA (SND, OPCA, PAF) and other parkinsonian syndromes (PD, PSP, and CBD) and cerebellar ataxias. These reports have generally involved small series of well-established cases analyzed in an open fashion without pathological confirmation of the clinical diagnosis though follow up has occasionally been available. Given this, the true sensitivity and specificity of FDG PET for diagnosing MSA in early cases and discriminating this disorder from other parkinsonian syndromes and ataxias remain difficult to estimate.

Fulham et al.<sup>54</sup> examined the value of FDG PET for discriminating between 30 patients with MSA and 15 with PAF. The MSA group comprised 8 MSA-C, 7 MSA-P, and 15 MSA patients with both cerebellar and parkinsonian features. The MSA but not the PAF patients showed reduced regional cerebral glucose metabolism (rCMRglc) in the cerebellum, brainstem, striatum, and frontal cortical regions. These workers concluded that FDG PET clearly distinguished MSA from PAF.

Gilman et al.<sup>55</sup> studied patterns of rCMRglc in patients with MSA, sporadic (sOPCA), and dominantly inherited (dOPCA) olivopontocerebellar atrophy. MSA and sOPCA cases both showed reduced rCMRglc in the brainstem, cerebellum, putamen, thalamus, and cerebral cortex. By contrast, dOPCA cases had decreased rCMRglc in the brainstem and cerebellum alone. The authors concluded that these findings were consistent with the possibility that, in many cases, sOPCA will evolve into MSA.

FDG PET studies in levodopa-nonresponsive akinetic-rigid patients with clinically probable SND have reported reduced levels of striatal glucose metabolism—in contrast with PD where striatal metabolism is preserved. Eidelberg reported that 8 of 10 probable SND cases showed reduced striatal metabolism, whereas this was normal or raised in levodopa-responsive PD cases.<sup>56</sup> De Volder et al. studied 7 cases of probable striatonigral degeneration, 2 of which had additional autonomic failure and cerebellar ataxia and so had the full syndrome of MSA.<sup>57</sup> They found reduced mean levels of putamen and caudate glucose metabolism and cerebellar metabolism was also reduced in the 2 patients with ataxia. Otsuka et al.<sup>58</sup> reported FDG PET findings in 9 patients with MSA and 15 with IPD. Five of the MSA patients had OPCA and 4 had SND. In MSA, rCMRglc was decreased in the striatum, cerebellum, brainstem, frontal, and temporal regions though there was an overlap between MSA and normal control ranges. Striatal metabolism was preserved in PD.

Eckert et al. have assessed the utility of FDG PET in the differential diagnosis of 135 parkinsonian patients.<sup>59</sup> Individual PET scans were assessed both visually and using statistical parametric maps (SPMs) of significant reductions in rCMRglc. The results were compared with 2-year follow-up clinical assessments made by independent movement disorders specialists blinded to the original PET findings. Blinded assessment of SPMs agreed with clinical diagnosis in 92.4% of all subjects (96% concordance in MSA), whereas visual inspection concurred with clinical diagnosis in 85.4% of the patients scanned (76% concordance in MSA). FDG PET performed at the time of initial referral for Parkinsonism accurately predicted the clinical diagnosis of MSA in individual patients confirmed at subsequent follow-up provided computer-assisted image analysis was available. Diagnoses based on visual analysis were less reliable.

#### Perfusion SPECT Studies

Bosman et al. have evaluated the contribution of brain perfusion ECD SPECT with anatomical standardization and automated analysis in the differentiation of PD and MSA.<sup>60</sup> SPECT was performed on 140 subjects: 81 PD and 15 MSA patients and only putamen perfusion differentiated MSA and PD, imaging providing correct classification (on clinical criteria) of MSA with a sensitivity of 73.3%, a specificity of 84%, and an accuracy of 83.6%.

The same group has subsequently combined ECD SPECT with statistical parametric mapping to improve its diagnostic accuracy.<sup>61</sup> In contrast to MSA, PD patients as a group showed significant reductions in frontal and temporal perfusion.

Network analysis has been used to identify a reproducible pattern of regional metabolic covariation in FDG PET scans that is associated with idiopathic PD.<sup>62</sup> The expression of this PD-related pattern (PDRP) can be quantified in individual subjects and used to discriminate PD patients from healthy controls and atypical cases. Feigin et al. have applied network analysis to <sup>99m</sup>Tc-ECD SPECT findings in PD and MSA.<sup>63</sup> PDRP values for one-third of individual subjects overlapped between the PD and MSA groups and the authors questioned the clinical utility of this method in the differential diagnosis of Parkinsonism.

Cilia et al.<sup>64</sup> measured brain flow with ECD SPECT in 36 MSA patients and compared this with 43 PD and 39 age-matched controls. Applying SPM, they found areas of significant reduced perfusion in the striatum, brainstem, and cerebellum in MSA compared with the other groups.

#### Proton Magnetic Resonance Spectroscopy

Proton magnetic resonance spectroscopy (PMRS) is a potential means of discriminating SND from PD. *N*-acetylaspartate (NAA) is found in high concentrations in neurons and is believed to be a metabolic marker of neuronal integrity. Davie et al.<sup>65</sup> initially reported reduced NAA/creatine (Cr) ratios in the proton MRS signal from the LN in 6 of 7 clinically probable SND cases, whereas 8 of 9 probable PD cases showed normal levels of putamen NAA. When Federico et al. studied 19 PD and 14 MSA cases, however, they found 50% of subjects in these cohorts had overlapping lentiform NAA/Cr ratios although the MSA group as a whole showed a significantly greater mean reduction.<sup>66</sup> Clarke and Lowry<sup>67</sup> reviewed 11 PMRS studies and concluded that changes in lentiform NAA/Cr signals were inconsistent in PD and MSA and could not be used as a reliable means of separating typical from atypical parkinsonian disorders.

Recently, Watanabe et al. have demonstrated that NAA/Cr signals are more reduced in the pons than in the LN of MSA-P cases.<sup>68</sup> By combining these measures, 8 of 11 MSA-P cases could be separated from 11 PD cases.

#### Pre- and Postsynaptic Dopaminergic Imaging

Pre- and postsynaptic dopaminergic function can be examined with both PET and SPECT. Dopamine storage capacity is reflected by <sup>18</sup>F-dopa uptake, vesicular monoamine transporter (VMAT2) function by <sup>11</sup>C-dihydrotrabenzazine (DTBZ) binding, and dopamine transporter binding by <sup>11</sup>C-nomifensine, <sup>123</sup>I-β-CIT, <sup>123</sup>I-FP-CIT, and <sup>99m</sup>Tc-TRODAT-1 uptake. Dopamine D1 binding has been imaged with <sup>11</sup>C-SCH23390 PET and D2 receptor binding with <sup>11</sup>C-raclopride PET and <sup>123</sup>I-IBZM, <sup>123</sup>I-epidepride, and <sup>123</sup>I-IBF SPECT.

#### Presynaptic Dopaminergic Imaging

In patients with clinically probable MSA-P, the function of the presynaptic dopaminergic systems is severely impaired. As in PD, putamen <sup>18</sup>F-dopa uptake is reduced to around 50% of normal levels in established MSA-P and individual levels of putamen <sup>18</sup>F-dopa uptake correlate with locomotor status.<sup>69,70</sup> Mean caudate <sup>18</sup>F-dopa uptake is significantly more depressed in MSA-P than in PD though the ranges overlap in 50% of individuals. Burn et al.<sup>71</sup> applied discriminant analysis to putamen and caudate <sup>18</sup>F-dopa uptake in patients with parkinsonian syndromes and found that patients were assigned to MSA, IPD, and

PSP groups with equal frequency. In contrast, Otsuka et al. reported  $^{18}\text{F}$ -dopa PET findings in 9 patients with MSA (5 MSA-C and 4 MSA-P) and 15 with PD. Caudate and putamen  $^{18}\text{F}$ -dopa uptake was impaired in both groups but the caudate-putamen index (CPI) reflecting differences in the uptakes in the caudate and putamen divided by the caudate uptake was  $5.6 \pm 4.6$  in the MSA patients and  $14.8 \pm 5.4$  in the PD patients, reflecting relatively greater caudate involvement in MSA. These workers concluded the  $^{18}\text{F}$ -dopa CPI can be helpful in discriminating MSA from PD.

Rinne et al.<sup>72</sup> examined 10 sOPCA patients with  $^{18}\text{F}$ -dopa PET. Mean putamen  $^{18}\text{F}$ -dopa uptake was significantly diminished to 71% of the control mean and individually 7 patients had significantly reduced uptake. These workers concluded that subclinical nigrostriatal dysfunction occurs in a majority of patients with sOPCA, in accordance with its status as part of the spectrum of MSA. Gilman et al.<sup>73</sup> used PET with racemic  $^{11}\text{C}$ -DTBZ to examine striatal VMAT2 binding in 4 MSA and 8 sOPCA patients. Specific caudate and putamen binding were significantly reduced in MSA with average reductions of 61% in the caudate and 58% in the putamen. Smaller reductions were found in sOPCA (26% in the caudate and 24% in the putamen). The finding of reduced striatal VMAT2 binding in sOPCA suggested subclinical nigrostriatal pathology. In a follow-up study, Gilman et al.<sup>73</sup> used the active (+) enantiomer of  $^{11}\text{C}$ -DTBZ with PET to study 8 MSA-P, 8 MSA-C, and 6 sOPCA patients. Again, VMAT2 binding was significantly reduced in the putamen of all patient groups.

Pirker et al.<sup>74</sup> used  $^{123}\text{I}$ - $\beta$ -CIT SPECT to study the pattern of dopamine transporter (DAT) binding in 18 patients with probable MSA (3 MSA-C, 15 MSA-P), 8 patients with PSP, 4 patients with corticobasal degeneration (CBD), and 48 patients with PD, and a similar degree of disability. They found that striatal DAT binding was significantly reduced in MSA (-51% of normal mean), PSP (-60%), CBD (-35%), and PD (-58%), without any overlap with control values. Asymmetry of striatal  $^{123}\text{I}$ - $\beta$ -CIT binding was significantly increased in patients with CBD and PD, and was less pronounced in MSA and PSP; however, the authors could not reliably discriminate these parkinsonian syndromes on the basis of SPECT. Kim et al.<sup>75</sup> came to a similar conclusion after studying 18 PD, 7 MSA-P, and 6 PSP patients with  $^{123}\text{I}$ - $\beta$ -CIT SPECT.

$^{99\text{m}}\text{Tc}$ -TRODAT-1 SPECT imaging has recently been used to compare striatal DAT binding in 30 MSA-P, 19 MSA-C, and 36 PD cases.<sup>76</sup> The authors

concluded that  $^{99\text{m}}\text{Tc}$ -TRODAT-1 SPECT can discriminate PD and MSA from normal and MSA-C from MSA-P but not MSA-P from PD reliably.

By investigating the integrity of the dopaminergic system with SPM and  $^{123}\text{I}$ - $\beta$ -CIT SPECT within the entire brain volume in patients with MSA-P, Scherfler et al.<sup>77</sup> and Seppi et al.<sup>78</sup> found similar reductions in striatal DAT activity in 15 patients with early MSA-P, 14 patients with PSP, and 17 patients with PD versus 13 controls to those detected using a standard ROI approach, but in addition, objectively localised focal reductions of  $^{123}\text{I}$ - $\beta$ -CIT signal in brainstem regions in MSA-P (59%) and PSP (52%) compared with both controls and PD patients, which could not have been predicted by visual inspection or ROI analysis of  $^{123}\text{I}$ - $\beta$ -CIT SPECT images. By using a midbrain mean specific-to-nondisplaceable equilibrium partition coefficient ( $V_3''$ ) of 2.3, 1 PD patient was classified as having atypical Parkinsonism, and one of the MSA-P patients as well as 2 of the PSP patients were classified as having PD. Patients with MSA-P and PSP could not be differentiated.

### Postsynaptic Dopaminergic Imaging

Studies of D2 dopamine receptor binding in PD with the most extensively used modalities,  $^{11}\text{C}$ -raclopride PET and  $^{123}\text{I}$ -IBZM SPECT, have shown a relative 10 to 20% increase of D2 binding in the putamen of early untreated patients contralateral to the more affected body side.<sup>72,79,80</sup> As PD advances and patients are exposed to dopaminergic agents,  $^{11}\text{C}$ -raclopride PET suggests that putamen D2 binding normalizes,<sup>79,81</sup> whereas  $^{123}\text{I}$ -IBZM SPECT and  $^{11}\text{C}$ -methylspiperone PET series suggest it may become subnormal.<sup>82-84</sup>

In contrast, in atypical parkinsonian syndromes,  $^{11}\text{C}$ -raclopride PET and  $^{123}\text{I}$ -IBZM SPECT suggest that D2 receptor density can be reduced from the onset of clinical symptoms.<sup>85,86</sup> Schwarz et al.<sup>86</sup> noted that two-thirds of their apomorphine nonresponsive parkinsonian patients with presumed SND had reduced levels of striatal  $^{123}\text{I}$ -IBZM uptake. Kim et al. found that 71% of their established MSA-P cases showed significantly reduced striatal  $^{123}\text{I}$ -IBF binding, whereas all their PD cases had normal or raised D2 availability.<sup>75</sup>

Although a combination of pre- and postsynaptic imaging markers of dopaminergic function (DAT and D2 receptor SPECT studies) has been suggested to result in increased sensitivity for the discrimination of PD and MSA, Knudsen et al. were only able to discriminate 2 of 8 MSA-P cases (all receiving dopaminergic drugs) from their 14 PD cases (3 drug naïve)

with such an approach.<sup>87</sup> In their series, PD and MSA cases showed equivalent reductions in striatal <sup>123</sup>I-β-CIT uptake allowing for disease severity but side-to-side asymmetry was greater in PD. Striatal D2 binding, measured with <sup>123</sup>I-epidepride SPECT, was raised above the PD range in 2 of the MSA-P cases.

Ghaemi et al.<sup>39</sup> compared the ability of multitracer PET with <sup>18</sup>F-dopa, FDG, and <sup>11</sup>C-raclopride to discriminate between PD and MSA-P patients. Seven healthy controls, 9 patients with a diagnosis of MSA-P, and 24 patients with a diagnosis of PD were recruited for the study. Both patient groups showed similar decreases in putaminal <sup>18</sup>F-dopa storage. Decreases of putaminal glucose metabolism and post-synaptic dopamine receptor density were found in the MSA-P group, but not in levodopa-responsive PD group. Putaminal FDG-PET and MRV proved equally capable of discriminating MSA-P from PD with the smallest overlap of individual data. However, 2 patients with MSA-P had putaminal FDG-PET values within the range of the PD group and 1 patient with MSA-P had a putaminal volume on MRV within the range of the PD group.

Plotkin et al. examined 72 consecutive cases of Parkinsonism with <sup>123</sup>I-FP-CIT and <sup>123</sup>I-IBZM SPECT.<sup>88</sup> On clinical follow-up, 25 were felt to have PD (12 drug naïve at the time of SPECT) and 13 to have MSA-P (6 drug naïve at the time of SPECT). <sup>123</sup>I-FP-CIT SPECT separated all PD and MSA-P cases from normal and essential tremor cases and reductions in mean striatal DAT binding were similar. Seven of the 13 (54%) MSA cases had reduced striatal D2 availability, whereas all PD cases had normal <sup>123</sup>I-IBZM uptake. The authors concluded that one could not confidently exclude MSA if <sup>123</sup>I-IBZM SPECT findings were normal.

Seppi et al.<sup>15</sup> have used <sup>123</sup>I-IBZM SPECT to objectively longitudinally monitor striatal degeneration in a group of early MSA cases. They found an annual 10% loss of striatal D2 binding in their 18-month study and concluded that <sup>123</sup>I-IBZM SPECT provides a valid future approach for testing the efficacy of putative neuroprotective agents in MSA. In another study, these workers compared the predictive accuracy of DWI and IBZM SPECT in discriminating MSA from PD. Striatal ADC levels separated 97% of MSA cases compared with a 75% separation with D2R binding levels suggesting that DWI may be more accurate compared with IBZM SPECT in the differential diagnosis of MSA-P versus PD.

Striatal dopamine D1 binding has been studied with PET in SND. Mild, but significant, reductions in mean

putamen <sup>11</sup>C-SCH23390 uptake have been reported though a wide overlap between SND, normal, and PD ranges was evident.<sup>89</sup>

### Imaging Opioid Binding and Glial Activation

The basal ganglia are rich in opioid peptides and binding sites and these are differentially affected in SND and PD. <sup>11</sup>C-diprenorphine is a nonspecific opioid antagonist binding with equal affinity for μ, κ, and δ sites. In nondyskinetic PD patients, caudate and putamen <sup>11</sup>C-diprenorphine uptake is preserved but becomes reduced in dyskinetic cases,<sup>90</sup> whereas putamen uptake is reduced in 50% of patients thought to have SND.<sup>91</sup>

<sup>11</sup>C-PK11195 PET, an in vivo marker of microglial activation, has been used to study neuroinflammatory changes in MSA.<sup>92</sup> Widespread subcortical increases in <sup>11</sup>C-PK11195 uptake were seen, particularly in nigra, putamen, pallidum, thalamus, and brainstem. Similar changes were evident in PD, though to a reduced extent.<sup>93</sup> Given this, neither <sup>11</sup>C-diprenorphine nor <sup>11</sup>C-PK11195 PET provides sensitive discriminators of MSA from PD.

### Imaging Cardiac Sympathetic Innervation

<sup>123</sup>I-metaiodobenzylguanidine (MIBG) is a norepinephrine analogue that is taken up and stored in sympathetic nerve endings. Multiple imaging studies with [<sup>123</sup>I]MIBG SPECT in PD patients have shown decreased cardiac uptake, indicating myocardial post-ganglionic sympathetic dysfunction<sup>94–97</sup> even where cardiovascular reflexes remain intact. However, in early stages of PD, MIBG uptake can be normal.<sup>98</sup> In most MIBG SPECT investigations of MSA, myocardial sympathetic innervation has been normal<sup>94,95,98,99</sup> though mildly reduced sympathetic innervation has been reported.<sup>96,100,101</sup> To summarize, MIBG SPECT will sensitively discriminate established PD from MSA-P as cardiac signals are reduced in the former and preserved in the latter; however, early PD may show normal cardiac sympathetic innervation and cannot reliably be discriminated from MSA.

Although investigations with MIBG SPECT have provided important information about peripheral autonomic involvement in IPD, the modality has several drawbacks. Commercial SPECT cameras have lower sensitivity and spatial resolution than PET cameras and quantitation relies on measuring the ratio of <sup>123</sup>I-MIBG cardiac to mediastinal activity. <sup>11</sup>C-metahydroxyephedrine (<sup>11</sup>C-MHED) PET can directly quantitate levels of myocardial sympathetic innervation.

TABLE 5. Structural and functional imaging in MSA

Structural imaging in MSA <sup>a</sup>	
Conventional MRI at 1.5 T	MSA cases may show low putamen, MCP, and brainstem signals and atrophy, and a hyperintense rim on T2 but these features, while supportive (especially versus PD), are not present in all cases and not specific versus other APDs.
MRI-based quantitative assessment of atrophy of different brain structures including MRI-based planimetry and volumetry	Quantitative MR measures of atrophy of different brain structures may help to distinguish MSA from PD (decreased MCP width in MSA; decreased putaminal volume in MSA-P) and PSP (decreased ratio of the area of the midbrain to the area of pons in patients with PSP), but neither of these specific studies have been reproduced.
Diffusion-weighted imaging (DWI)	DWI looks promising for separating atypical from typical PD showing increased diffusivity in the putamen. However, PSP patients can also show increased putaminal diffusivity. The finding of increased diffusivity in the MCP in patients with MSA versus PSP has to be reproduced by others.
Transcranial sonography (TCS)	TCS may be helpful in supporting a diagnosis of MSA as midbrain hyperechogenicity is usually absent, while 90% of PD cases show altered nigral signal. Separation between MSA and PSP patients is suboptimal for both SN and lentiform hyperechogenicity. Importantly, at least 10% of the population have a temporal bone window insufficient for an adequate brain parenchyma sonographic analysis.
Functional imaging in MSA	
Presynaptic dopaminergic imaging	Imaging presynaptic dopaminergic function with PET or SPECT reliably separates parkinsonian from nonparkinsonian conditions but does not allow discrimination of MSA from other parkinsonian conditions.
Postsynaptic dopaminergic imaging	MSA cases show reduced putamen dopamine D2 receptor binding, whereas this is normal or elevated in PD. However, the PD and MSA ranges overlap and one-third of MSA cases show normal D2 availability.
FDG PET	FDG PET can be helpful for discriminating typical from atypical PD, particularly when combined with computer-assisted statistical parametric mapping which increases the sensitivity relative to visual analysis from 80 to 95%. MSA cases show striatal, brainstem, and cerebellar hypometabolism while putamen metabolism is elevated and frontotemporal metabolism reduced in PD.
Imaging cardiac sympathetic innervation	Most PD cases show reduced myocardial sympathetic innervation with MIBG SPECT or <sup>18</sup> F-dopamine PET, whereas this is not seen in MSA or PSP; however, early PD may show normal cardiac sympathetic innervation and MSA may show reduced cardiac sympathetic innervation.

<sup>a</sup>Importantly, structural imaging was scarcely used in patients with MSA-C. It seems that signal changes at 1.5 T and atrophy in different brainstem regions (especially MCP and pons) on conventional MRI and reduced brainstem volume on MR-volumetry may help to differentiate patients with MSA-C from patients with idiopathic cerebellar ataxia with extracerebellar presentation not corresponding to MSA-C.

Berding et al.<sup>102</sup> have reported the results of a pilot study investigating 7 patients, 2 with MSA and 5 with PD (3 had orthostatic hypotension). Ratios of MHED uptake in the myocardium to the liver at 5 and 40 minutes postinjection were calculated. Compared with MSA, 4 of the 5 PD patients showed lower uptake ratios at both time points, those with OH having lowest myocardial signals.

Raffel et al. have reported MHED PET findings for 5 MSA, 2 PSP, and 10 normal subjects.<sup>103</sup> Two MSA patients had reduced cardiac MHED uptake, whereas the 3 remaining MSA patients and both PSP patients had normal imaging. The authors concluded that, although most MSA patients have normal cardiac post-ganglionic sympathetic innervation, severe denervation can be seen.

Goldstein et al.<sup>104</sup> employed <sup>18</sup>F-dopamine PET to examine the function of myocardial sympathetic innervation in subjects with and without dysautonomia. In their first series, 3 cases of pure autonomic failure showed severely reduced myocardial <sup>18</sup>F-dopamine

retention.<sup>104</sup> In contrast, 9 MSA patients with impaired cardiovascular reflexes (Shy-Drager syndrome) showed raised levels of myocardial sympathetic function, whereas MSA cases without sympathetic neuro-circulatory failure had normal <sup>18</sup>F-dopamine uptake. Their 2 cases of levodopa-responsive Parkinsonism with impaired cardiovascular reflexes showed no appreciable myocardial <sup>18</sup>F-dopamine uptake similar to PAF. The authors concluded that <sup>18</sup>F-dopamine PET could be used to classify dysautonomic syndromes into pre- and postganglionic syndromes.

In a follow-up series, these workers performed <sup>18</sup>F-dopamine PET on 29 cases of Parkinson's disease (9 with impaired cardiovascular reflexes), 24 cases of MSA (17 with impaired cardiovascular reflexes), and 7 cases of pure autonomic failure.<sup>105</sup> All 9 PD cases with orthostatic hypotension and another 11 without showed reduced myocardial <sup>18</sup>F-dopamine uptake to the low levels seen in pure autonomic failure cases. In contrast, all 24 cases of MSA had normal myocardial <sup>18</sup>F-dopamine retention. The authors again concluded

that most cases of PD, but not MSA, are associated with postganglionic sympathetic denervation of the myocardium.

### CONCLUSIONS

To summarize, the characteristic abnormalities shown by MSA cases with the different structural and functional neuroimaging methods have been documented for patients with an established clinical diagnosis (see Table 5). To determine which of these techniques will emerge as standard investigations in the work-up of MSA patients presenting requires further prospective studies during early disease stages when the clinical diagnosis remains uncertain. Based on the best current knowledge, the revised consensus criteria include neuroimaging criteria for the diagnostic category of possible MSA.<sup>103</sup> Atrophy on conventional MRI of putamen, MCP, pons, or cerebellum or hypometabolism on FDG-PET in putamen, brainstem, or cerebellum were included as additional features for possible MSA-P; and atrophy on conventional MRI of putamen, MCP, or pons or hypometabolism on FDG-PET in putamen were included as additional features for possible MSA-C.

**Acknowledgments:** The second consensus conference on multiple system atrophy (MSA) was supported in part by grants from the NIH (National Institute of Neurological Disorders and Stroke grant 1 R13 NS055459), Novartis Pharmaceuticals, and Chelsea Therapeutics, and the American Academy of Neurology (AAN) agreed to cosponsor the event. This manuscript was prepared for the conference by the Neuroimaging group of the second consensus conference, which included the authors of this manuscript DJB (Chair) and KS.

**Contributor Roles:** David Brooks: Conception; literature search and writing of the first draft, especially regarding the part of “Functional imaging in MSA”; review and critique of the whole manuscript.

Klaus Seppi: Conception; literature search and writing of the first draft, especially regarding the part of “Structural imaging in MSA”; review and critique of the whole manuscript.

### REFERENCES

- Konagaya M, Konagaya Y, Iida M. Clinical and magnetic resonance imaging study of extrapyramidal symptoms in multiple system atrophy. *J Neurol Neurosurg Psychiatry* 1994;57:1528–1531.
- Kraft E, Schwarz J, Trenkwalder C, Vogl T, Pfluger T, Oertel WH. The combination of hypointense and hyperintense signal changes on T2-weighted magnetic resonance imaging sequences: a specific marker of multiple system atrophy? *Arch Neurol* 1999;56:225–228.
- von Lewinski, Werner C, Jorn T, Mohr A, Sixel-Doring F, Trenkwalder C. T2\*-weighted MRI in diagnosis of multiple system atrophy. A practical approach for clinicians. *J Neurol* 2007;254:1184–1188.
- Righini A, Antonini A, Ferrarini M, et al. Thin section MR study of the basal ganglia in the differential diagnosis between striatonigral degeneration and Parkinson’s disease. *J Comput Assist Tomogr* 2002;26:266–271.
- Schocke MF, Seppi K, Esterhammer R, et al. Diffusion-weighted MRI differentiates the Parkinson variant of multiple system atrophy from PD. *Neurology* 2002;58:575–580.
- Lee EA, Cho HI, Kim SS, Lee WY. Comparison of magnetic resonance imaging in subtypes of multiple system atrophy. *Parkinsonism Relat Disord* 2004;10:363–368.
- Bhattacharya K, Saadia D, Eisenkraft B, et al. Brain magnetic resonance imaging in multiple-system atrophy and Parkinson’s disease: a diagnostic algorithm. *Arch Neurol* 2002;59:835–842.
- Burk K, Buhring U, Schulz JB, Zuhlke C, Hellenbroich Y, Dichgans J. Clinical and magnetic resonance imaging characteristics of sporadic cerebellar ataxia. *Arch Neurol* 2005;62:981–985.
- Nicoletti G, Fera F, Condino F, et al. MR imaging of middle cerebellar peduncle width: differentiation of multiple system atrophy from Parkinson’s disease. *Radiology* 2006;239:825–830.
- Paviour DC, Thornton JS, Lees AJ, Jager HR. Diffusion-weighted magnetic resonance imaging differentiates parkinsonian variant of multiple-system atrophy from progressive supranuclear palsy. *Mov Disord* 2007;22:68–74.
- Seppi K, Schocke MF, Prenschiuetz-Schuetzenau K, et al. Topography of putaminal degeneration in multiple system atrophy: a diffusion magnetic resonance study. *Mov Disord* 2006;21:847–852.
- Schulz JB, Skalej M, Wedekind D, et al. Magnetic resonance imaging-based volumetry differentiates idiopathic Parkinson’s syndrome from multiple system atrophy and progressive supranuclear palsy. *Ann Neurol* 1999;45:65–74.
- Burk K, Globas C, Wahl T, et al. MRI-based volumetric differentiation of sporadic cerebellar ataxia. *Brain* 2004;127(Part 1):175–181.
- Quattrone A, Nicoletti G, Messina D, et al. MR imaging index for differentiation of progressive supranuclear palsy from Parkinson’s disease and the Parkinson variant of multiple system atrophy. *Radiology* 2008;246:214–221.
- Seppi K, Schocke MF, Donnemiller E, et al. Comparison of diffusion-weighted imaging and [123I]IBZM-SPECT for the differentiation of patients with the Parkinson variant of multiple system atrophy from those with Parkinson’s disease. *Mov Disord* 2004;19:1438–1445.
- Schocke MF, Seppi K, Esterhammer R, et al. Trace of diffusion tensor differentiates the Parkinson variant of multiple system atrophy and Parkinson’s disease. *Neuroimage* 2004;21:1443–1451.
- Nicoletti G, Lodi R, Condino F, et al. Apparent diffusion coefficient measurements of the middle cerebellar peduncle differentiate the Parkinson variant of MSA from Parkinson’s disease and progressive supranuclear palsy. *Brain* 2006;129(Part 10):2679–2687.
- Ito M, Watanabe H, Kawai Y, et al. Usefulness of combined fractional anisotropy and apparent diffusion coefficient values for detection of involvement in multiple system atrophy. *J Neurol Neurosurg Psychiatry* 2007;78:722–728.
- Eckert T, Sailer M, Kaufmann J, et al. Differentiation of idiopathic Parkinson’s disease, multiple system atrophy, progressive supranuclear palsy, and healthy controls using magnetization transfer imaging. *Neuroimage* 2004;21:229–235.
- Walter U, Niehaus L, Probst T, Benecke R, Meyer BU, Dressler D. Brain parenchyma sonography discriminates Parkinson’s disease and atypical parkinsonian syndromes. *Neurology* 2003;60:74–77.

21. Behnke S, Berg D, Naumann M, Becker G. Differentiation of Parkinson's disease and atypical parkinsonian syndromes by transcranial ultrasound. *J Neurol Neurosurg Psychiatry* 2005; 76:423–425.
22. Okawa M, Miwa H, Kajimoto Y, et al. Transcranial sonography of the substantia nigra in Japanese patients with Parkinson's disease or atypical Parkinsonism: clinical potential and limitations. *Intern Med* 2007;46:1527–1531.
23. Walter U, Dressler D, Probst T, et al. Transcranial brain sonography findings in discriminating between Parkinsonism and idiopathic Parkinson's disease. *Arch Neurol* 2007;64:1635–1640.
24. Drayer BP, Olanow W, Burger P, Johnson GA, Herfkens R, Riederer S. Parkinson plus syndrome: diagnosis using high field MR imaging of brain iron. *Radiology* 1986;159:493–498.
25. Pastakia B, Polinsky R, Di CG, Simmons JT, Brown R, Wener L. Multiple system atrophy (Shy-Drager syndrome): MR imaging. *Radiology* 1986;159:499–502.
26. Schrag A, Kingsley D, Phatouros C, et al. Clinical usefulness of magnetic resonance imaging in multiple system atrophy. *J Neurol Neurosurg Psychiatry* 1998;65:65–71.
27. Schrag A, Good CD, Miszkil K, et al. Differentiation of atypical parkinsonian syndromes with routine MRI. *Neurology* 2000;54: 697–702.
28. Savoirdo M. Differential diagnosis of Parkinson's disease and atypical parkinsonian disorders by magnetic resonance imaging. *Neurol Sci* 2003;24(Suppl 1):S35–S37.
29. Seppi K, Schocke MF, Mair KJ, et al. Progression of putaminal degeneration in multiple system atrophy: a serial diffusion MR study. *Neuroimage* 2006;31:240–245.
30. Yekhlief F, Ballan G, Macia F, Delmer O, Sourgen C, Tison F. Routine MRI for the differential diagnosis of Parkinson's disease, MSA, PSP, and CBD. *J Neural Transm* 2003;110:151–169.
31. Ito S, Shirai W, Hattori T. Evaluating posterolateral linearization of the putaminal margin with magnetic resonance imaging to diagnose the Parkinson variant of multiple system atrophy. *Mov Disord* 2007;22:578–581.
32. Lee WH, Lee CC, Shyu WC, Chong PN, Lin SZ. Hyperintense putaminal rim sign is not a hallmark of multiple system atrophy at 3T. *AJNR Am J Neuroradiol* 2005;26:2238–2242.
33. Muqit MM, Mort D, Miskiel KA, Shakir RA. "Hot cross bun" sign in a patient with Parkinsonism secondary to presumed vasculitis. *J Neurol Neurosurg Psychiatry* 2001;71:565–566.
34. Burk K, Skalej M, Dichgans J. Pontine MRI hyperintensities ("the cross sign") are not pathognomonic for multiple system atrophy (MSA). *Mov Disord* 2001;16:535.
35. Watanabe H, Saito Y, Terao S, et al. Progression and prognosis in multiple system atrophy: an analysis of 230 Japanese patients. *Brain* 2002;125(Part 5):1070–1083.
36. Horimoto Y, Aiba I, Yasuda T, et al. Longitudinal MRI study of multiple system atrophy—when do the findings appear, and what is the course? *J Neurol* 2002;249:847–854.
37. Yabe I, Soma H, Takei A, Fujiki N, Yanagihara T, Sasaki H. MSA-C is the predominant clinical phenotype of MSA in Japan: analysis of 142 patients with probable MSA. *J Neurol Sci* 2006;249:115–121.
38. Kraft E, Trenkwalder C, Auer DP. T2\*-weighted MRI differentiates multiple system atrophy from Parkinson's disease. *Neurology* 2002;59:1265–1267.
39. Ghaemi M, Hilker R, Rudolf J, Sobesky J, Heiss WD. Differentiating multiple system atrophy from Parkinson's disease: contribution of striatal and midbrain MRI volumetry and multi-tracer PET imaging. *J Neurol Neurosurg Psychiatry* 2002;73: 517–523.
40. Brenneis C, Seppi K, Schocke MF, et al. Voxel-based morphometry detects cortical atrophy in the Parkinson variant of multiple system atrophy. *Mov Disord* 2003;18:1132–1138.
41. Specht K, Minnerop M, Abele M, Reul J, Wullner U, Klockgether T. In vivo voxel-based morphometry in multiple system atrophy of the cerebellar type. *Arch Neurol* 2003;60:1431–1435.
42. Brenneis C, Boesch SM, Egger KE, et al. Cortical atrophy in the cerebellar variant of multiple system atrophy: a voxel-based morphometry study. *Mov Disord* 2006;21:159–165.
43. Specht K, Minnerop M, Muller-Hubenthal J, Klockgether T. Voxel-based analysis of multiple-system atrophy of cerebellar type: complementary results by combining voxel-based morphometry and voxel-based relaxometry. *Neuroimage* 2005;25: 287–293.
44. Minnerop M, Specht K, Ruhlmann J, et al. Voxel-based morphometry and voxel-based relaxometry in multiple system atrophy—a comparison between clinical subtypes and correlations with clinical parameters. *Neuroimage* 2007;36:1086–1095.
45. Brenneis C, Egger K, Scherfler C, et al. Progression of brain atrophy in multiple system atrophy. A longitudinal VBM study. *J Neurol* 2007;254:191–196.
46. Oba H, Yagishita A, Terada H, et al. New and reliable MRI diagnosis for progressive supranuclear palsy. *Neurology* 2005; 64: 2050–2055.
47. Seppi K, Schocke MF, Esterhammer R, et al. Diffusion-weighted imaging discriminates progressive supranuclear palsy from PD, but not from the Parkinson variant of multiple system atrophy. *Neurology* 2003;60:922–927.
48. Naka H, Imon Y, Ohshita T, et al. Magnetization transfer measurements of brain structures in patients with multiple system atrophy. *Neuroimage* 2002;17:1572–1578.
49. Kanazawa M, Shimohata T, Terajima K, et al. Quantitative evaluation of brainstem involvement in multiple system atrophy by diffusion-weighted MR imaging. *J Neurol* 2004;251:1121–1124.
50. Blain CR, Barker GJ, Jarosz JM, et al. Measuring brain stem and cerebellar damage in parkinsonian syndromes using diffusion tensor MRI. *Neurology* 2006;67:2199–2205.
51. Berg D, Siefker C, Becker G. Echogenicity of the substantia nigra in Parkinson's disease and its relation to clinical findings. *J Neurol* 2001;248:684–689.
52. Stockner H, Seppi K, Kiechl S, et al. Midbrain transcranial sonography findings in a population-based study. *Mov Disord* 2006;25(Suppl):S634 (Abstract).
53. Schmidauer C, Sojer M, Seppi K, et al. Transcranial ultrasound shows nigral hypoechoogenicity in restless legs syndrome. *Ann Neurol* 2005;58:630–634.
54. Fulham MJ, Dubinsky RM, Polinsky RJ, et al. Computed tomography, magnetic resonance imaging and positron emission tomography with [<sup>18</sup>F]fluorodeoxyglucose in multiple system atrophy and pure autonomic failure. *Clin Auton Res* 1991; 1:27–36.
55. Gilman S, Koeppe RA, Junck L, Klun KJ, Lohman M, St Laurent RT. Patterns of cerebral glucose metabolism detected with positron emission tomography differ in multiple system atrophy and olivopontocerebellar atrophy. *Ann Neurol* 1994;36:166–175.
56. Eidelberg D, Takikawa S, Moeller JR, et al. Striatal hypometabolism distinguishes striatonigral degeneration from Parkinson's disease. *Ann Neurol* 1993;33:518–527.
57. De Volder AG, Francart J, Laterre C, et al. Decreased glucose utilization in the striatum and frontal lobe in probable striatonigral degeneration. *Ann Neurol* 1989;26:239–247.
58. Otsuka M, Kuwabara Y, Ichiya Y, et al. Differentiating between multiple system atrophy and Parkinson's disease by positron emission tomography with 18F-dopa and 18F-FDG. *Ann Nucl Med* 1997;11:251–257.
59. Eckert T, Barnes A, Dhawan V, et al. FDG PET in the differential diagnosis of parkinsonian disorders. *Neuroimage* 2005; 26:912–921.
60. Bosman T, Van LK, Santens P. Anatomically standardised 99mTc-ECD brain perfusion SPET allows accurate differentiation between healthy volunteers, multiple system atrophy and

- idiopathic Parkinson's disease. *Eur J Nucl Med Mol Imaging* 2003; 30:16–24.
61. Van LK, Santens P, Bosman T, De RJ, Mortelmans L, Dierckx R. Statistical parametric mapping of (99m)Tc-ECD SPECT in idiopathic Parkinson's disease and multiple system atrophy with predominant parkinsonian features: correlation with clinical parameters. *J Nucl Med* 2004;45:933–942.
  62. Eidelberg D, Moeller JR, Ishikawa T, et al. Assessment of disease severity in Parkinsonism with fluorine-18-fluorodeoxyglucose and PET. *J Nucl Med* 1995;36:378–383.
  63. Feigin A, Antonini A, Fukuda M, et al. Tc-99m ethylene cysteine dimer SPECT in the differential diagnosis of Parkinsonism. *Mov Disord* 2002;17:1265–1270.
  64. Cilia R, Marotta G, Benti R, Pezzoli G, Antonini A. Brain SPECT imaging in multiple system atrophy. *J Neural Transm* 2005;112:1635–1645.
  65. Davie CA, Wenning GK, Barker GJ, et al. Differentiation of multiple system atrophy from idiopathic Parkinson's disease using proton magnetic resonance spectroscopy. *Ann Neurol* 1995;37:204–210.
  66. Federico F, Simone IL, Lucivero V, et al. Usefulness of proton magnetic resonance spectroscopy in differentiating parkinsonian syndromes. *Ital J Neurol Sci* 1999;20:223–229.
  67. Clarke CE, Lowry M. Systematic review of proton magnetic resonance spectroscopy of the striatum in parkinsonian syndromes. *Eur J Neurol* 2001;8:573–577.
  68. Watanabe H, Fukatsu H, Katsuno M, et al. Multiple regional 1H-MR spectroscopy in multiple system atrophy: NAA/Cr reduction in pontine base as a valuable diagnostic marker. *J Neurol Neurosurg Psychiatry* 2004;75:103–109.
  69. Brooks DJ, Salmon EP, Mathias CJ, et al. The relationship between locomotor disability, autonomic dysfunction, and the integrity of the striatal dopaminergic system in patients with multiple system atrophy, pure autonomic failure, and Parkinson's disease, studied with PET. *Brain* 1990;113(Part 5):1539–1552.
  70. Brooks DJ, Ibanez V, Sawle GV, et al. Differing patterns of striatal 18F-dopa uptake in Parkinson's disease, multiple system atrophy, and progressive supranuclear palsy. *Ann Neurol* 1990;28:547–555.
  71. Burn DJ, Sawle GV, Brooks DJ. Differential diagnosis of Parkinson's disease, multiple system atrophy, and Steele-Richardson-Olszewski syndrome: discriminant analysis of striatal 18F-dopa PET data. *J Neurol Neurosurg Psychiatry* 1994;57:278–284.
  72. Rinne JO, Burn DJ, Mathias CJ, Quinn NP, Marsden CD, Brooks DJ. Positron emission tomography studies on the dopaminergic system and striatal opioid binding in the olivopontocerebellar atrophy variant of multiple system atrophy. *Ann Neurol* 1995;37:568–573.
  73. Gilman S, Frey KA, Koeppe RA, et al. Decreased striatal monoaminergic terminals in olivopontocerebellar atrophy and multiple system atrophy demonstrated with positron emission tomography. *Ann Neurol* 1996;40:885–892.
  74. Pirker W, Asenbaum S, Bencsits G, et al. [123I]β-CIT SPECT in multiple system atrophy, progressive supranuclear palsy, and corticobasal degeneration. *Mov Disord* 2000;15:1158–1167.
  75. Kim YJ, Ichise M, Ballinger JR, et al. Combination of dopamine transporter and D2 receptor SPECT in the diagnostic evaluation of PD, MSA, and PSP. *Mov Disord* 2002;17:303–312.
  76. Lu CS, Weng YH, Chen MC, et al. 99mTc-TRODAT-1 imaging of multiple system atrophy. *J Nucl Med* 2004;45:49–55.
  77. Scherfler C, Seppi K, Donnemiller E, et al. Voxel-wise analysis of [123I]β-CIT SPECT differentiates the Parkinson variant of multiple system atrophy from idiopathic Parkinson's disease. *Brain* 2005;128(Part 7):1605–1612.
  78. Seppi K, Scherfler C, Donnemiller E, et al. Topography of dopamine transporter availability in progressive supranuclear palsy: a voxelwise [123I]β-CIT SPECT analysis. *Arch Neurol* 2006;63:1154–1160.
  79. Antonini A, Schwarz J, Oertel WH, Beer HF, Madeja UD, Leenders KL. [11C]raclopride and positron emission tomography in previously untreated patients with Parkinson's disease: influence of L-dopa and lisuride therapy on striatal dopamine D2-receptors. *Neurology* 1994;44:1325–1329.
  80. Kaasinen V, Nagren K, Hietala J, et al. Extrastriatal dopamine D2 and D3 receptors in early and advanced Parkinson's disease. *Neurology* 2000;54:1482–1487.
  81. Turjanski N, Lees AJ, Brooks DJ. In vivo studies on striatal dopamine D1 and D2 site binding in L-dopa-treated Parkinson's disease patients with and without dyskinesias. *Neurology* 1997; 49:717–723.
  82. Pizzolato G, Chierichetti F, Rossato A, et al. Alterations of striatal dopamine D2 receptors contribute to deteriorated response to L-dopa in Parkinson's disease: a [123I]-IBZM SPET study. *J Neural Transm Suppl* 1995;45:113–122.
  83. Hwang WJ, Yao WJ, Wey SP, Shen LH, Ting G. Downregulation of striatal dopamine D2 receptors in advanced Parkinson's disease contributes to the development of motor fluctuation. *Eur Neurol* 2002;47:113–117.
  84. Shinotoh H, Aotsuka A, Yonezawa H. Striatal dopamine D2 receptors in Parkinson's disease and striato-nigral degeneration determined by positron emission tomography. In: Nagatsu T, Fisher A, Yoshida M, editors. *Basic, clinical and therapeutic advances of Alzheimer's and Parkinson's diseases*, Vol. 2. New York: Plenum Press; 1990. p 107–110.
  85. van RE, Verhoeff NF, Speelman JD, Wolters EC, Kuiper MA, Janssen AG. Multiple system atrophy and progressive supranuclear palsy diminished striatal D2 dopamine receptor activity demonstrated by 123I-IBZM single photon emission computed tomography. *Arch Neurol* 1993;50:513–516.
  86. Schwarz J, Tatsch K, Arnold G, et al. 123I-iodobenzamide-SPECT predicts dopaminergic responsiveness in patients with de novo Parkinsonism. *Neurology* 1992;42(3 Part 1): 556–561.
  87. Knudsen GM, Karlsborg M, Thomsen G, et al. Imaging of dopamine transporters and D2 receptors in patients with Parkinson's disease and multiple system atrophy. *Eur J Nucl Med Mol Imaging* 2004;31:1631–1638.
  88. Plotkin M, Amthauer H, Klaffke S, et al. Combined 123I-FP-CIT and 123I-IBZM SPECT for the diagnosis of parkinsonian syndromes: study on 72 patients. *J Neural Transm* 2005;112: 677–692.
  89. Shinotoh H, Inoue O, Hirayama K, et al. Dopamine D1 receptors in Parkinson's disease and striatonigral degeneration: a positron emission tomography study. *J Neurol Neurosurg Psychiatry* 1993;56:467–472.
  90. Piccini P, Weeks RA, Brooks DJ. Alterations in opioid receptor binding in Parkinson's disease patients with levodopa-induced dyskinesias. *Ann Neurol* 1997;42:720–726.
  91. Burn DJ, Rinne JO, Quinn NP, Lees AJ, Marsden CD, Brooks DJ. Striatal opioid receptor binding in Parkinson's disease, striatonigral degeneration and Steele-Richardson-Olszewski syndrome. A [11C]diprenorphine PET study. *Brain* 1995;118 (Part 4):951–958.
  92. Gerhard A, Banati RB, Goerres GB, et al. [11C](R)-PK11195 PET imaging of microglial activation in multiple system atrophy. *Neurology* 2003;61:686–689.
  93. Gerhard A, Pavese N, Hotton G, et al. In vivo imaging of microglial activation with [11C](R)-PK11195 PET in idiopathic Parkinson's disease. *Neurobiol Dis* 2006;21:404–412.
  94. Takatsu H, Nagashima K, Murase M, et al. Differentiating Parkinson's disease from multiple-system atrophy by measuring cardiac iodine-123 metaiodobenzylguanidine accumulation. *JAMA* 2000;284:44–45.

95. Reinhardt MJ, Jungling FD, Krause TM, Braune S. Scintigraphic differentiation between two forms of primary dysautonomia early after onset of autonomic dysfunction: value of cardiac and pulmonary iodine-123 MIBG uptake. *Eur J Nucl Med* 2000;27:595–600.
96. Druschky A, Hilz MJ, Platsch G, et al. Differentiation of Parkinson's disease and multiple system atrophy in early disease stages by means of I-123-MIBG-SPECT. *J Neurol Sci* 2000;175: 3–12.
97. Courbon F, Brefel-Courbon C, Thalamas C, et al. Cardiac MIBG scintigraphy is a sensitive tool for detecting cardiac sympathetic denervation in Parkinson's disease. *Mov Disord* 2003; 18:890–897.
98. Satoh A, Serita T, Seto M, et al. Loss of 123I-MIBG uptake by the heart in Parkinson's disease: assessment of cardiac sympathetic denervation and diagnostic value. *J Nucl Med* 1999;40: 371–375.
99. Braune S, Reinhardt M, Schnitzer R, Riedel A, Lucking CH. Cardiac uptake of [123I]MIBG separates Parkinson's disease from multiple system atrophy. *Neurology* 1999;53:1020–1025.
100. Yoshita M. Differentiation of idiopathic Parkinson's disease from striatonigral degeneration and progressive supranuclear palsy using iodine-123 meta-iodobenzylguanidine myocardial scintigraphy. *J Neurol Sci* 1998;155:60–67.
101. Hirayama M, Hokusui S, Koike Y, et al. A scintigraphical qualitative analysis of peripheral vascular sympathetic function with meta-[123I]iodobenzylguanidine in neurological patients with autonomic failure. *J Auton Nerv Syst* 1995;53: 230–234.
102. Berding G, Brucke T, Odin P, et al. [[123I]β-CIT SPECT imaging of dopamine and serotonin transporters in Parkinson's disease and multiple system atrophy. *Nuklearmedizin* 2003;42: 31–38.
103. Raffel DM, Koeppe RA, Little R et al. PET measurement of cardiac and nigrostriatal denervation in Parkinsonian syndromes. *J Nucl Med*. 2006;47:1769–1777.
104. Goldstein DS, Holmes C, Cannon RO, III, Eisenhofer G, Kopin IJ. Sympathetic cardioneuropathy in dysautonomias. *N Engl J Med* 1997;336:696–702.
105. Goldstein DS, Holmes C, Li ST, Bruce S, Metman LV, Cannon RO, III. Cardiac sympathetic denervation in Parkinson's disease. *Ann Intern Med* 2000;133:338–347.